2016

Method for Determining Air Side Convective Heat Transfer Coefficient Using Infrared Thermography

Scott S. Wujek
Creative Thermal Solutions, United States of America, scott.wujek@creativethermalsolutions.com

Wayne L. Staats
Sandia National Laboratory, United States of America, wstaats@sandia.gov

Stefan W. Elbel
Creative Thermal Solutions, United States of America, stefan.elbel@creativethermalsolutions.com

Jeffrey P. Koplow
Sandia National Laboratory, United States of America, jkoplow@sandia.gov

H. Arthur Kariya
Sandia National Laboratory, United States of America, hakariy@sandia.gov

See next page for additional authors

Method for Determining Air Side Convective Heat Transfer Coefficient Using Infrared Thermography

Scott S. Wujek[1]*, Wayne L. Staats[2], Stefan W. Elbel[1],
Jeffrey P. Koplow[2], H. Arthur Kariya[2], Predrag S. Hrnjak[1]

[1]Creative Thermal Solutions
Urbana, Illinois, United States of America
scott.wujek@creativethermalsolutions.com

[2]Sandia National Laboratories
Livermore, California, United States of America

* Corresponding Author

ABSTRACT

Air side convective heat transfer coefficients are among the most important parameters to know when modeling thermal systems due to their dominant impact on the overall heat transfer coefficient. Local air side convective heat transfer coefficients can often prove challenging to measure experimentally due to limitations with sensor accuracy, complexity of surface geometries, and changes to the heat transfer due to the installation of the sensor itself. Infrared thermography allows local heat transfer coefficients to be accurately determined for many different surface geometries in a non-intrusive manner which does not impact the results. Moreover, when determining convective heat transfer coefficients for a large number of samples, it is less costly in terms of both time and materials than other experimental methods.

Using infrared thermography, we report a method that determines the heat transfer coefficient for an arbitrary region by determining the rate at which the surface temperature changes due to a step change in air temperature. To utilize the method a simple calibration is first done to determine the local thermal time constant under natural convection. Alternatively, if the thermal properties of the object are well known, a model may be used. In subsequent tests, the ratio of thermal time constant to that from the calibration test can be determined. As the material properties of the solid object are unchanged, the convective heat transfer coefficient scales nearly inversely with the thermal time constant. A computer script was created which automates the entire analysis process with the exception of determining the region of interest. Using this method, real-time heat transfer coefficient measurements of were performed rotating fan blade.

1. INTRODUCTION

The convective heat transfer coefficient (h) is the proportionality constant in Newton's Law of Cooling, given by Equation 1, which relates convective heat flux (q'') to the body's surface temperature (T_s) and the bulk fluid temperature (T_∞). The convective heat transfer coefficient may be defined either locally or as averaged over an area. The convective heat transfer coefficient is generally a function of fluid properties, flow conditions, and surface geometry.

$$q'' = h(T_s - T_\infty) \tag{1}$$

The form of the heat transfer equation guides the methodology used to measure the convective heat transfer coefficient. To determine convective heat transfer coefficients, the other three parameters in the equation must be

measured simultaneously: the temperature of the fluid (air), the surface temperature of the solid body, and the heat flux. Heat flux is generally determined by knowing the total amount of heat applied and dividing by the surface area. The amount of heat applied is generally measured in one of two main ways: measuring the electrical power supplied to a resistive heater or calculated from specific heat, mass, and a temperature change. Often, the latter is done by incorporating a single phase fluid flowing within the body at a steady rate and undergoing a steady temperature change. Dedicated heat flux sensors are also commercially available, these generally consist of a thermopile attached onto both surfaces of a thin sheet of known thickness and material properties.

Various methods for measuring air-side convective heat transfer have been employed by many researchers especially for stationary applications. However, for certain applications, such as those with rotational movement, many of these methods are ill-suited. The act of rotation hinders the use of many electronic based measurements because slip rings or wireless measurement equipment are required. Both of which become challenging when local heat transfer is of interest as channel counts grow proportionally with the number of regions of interest. Likewise several optical based methods have been employed, but many of these are ill suited for high speed rotation or when the driving temperature differences are relatively small. Finally, many of these experiments are very expensive in terms of time and labor to prepare and many of these costs are recurring costs which are incurred each time a new geometry is employed. This is because there is the need to apply many film type heaters, rewire measurement devices, and recalibrate instrumentation. Despite these difficulties heat transfer research was done as part of NASA's HOST program in the late 1980s to study jet turbine engines. Blair and Anderson (1989) attached an electrically heated skin onto a rigid foam castings of turbine airfoils. The heater power and the surface temperature was measured with a combination of thermocouples and sprayed thermochromatic liquid crystals. The liquid crystals used has color changes that occurred at well-known temperatures (within 1.1°C or 2°F), temperature was determined with an SLR camera with high speed color film. Gluing a wrinkle-free metal foil to the foam was reportedly difficult. The temperature transition pattern in the liquid crystals was also not discernable when using a roughened surface.

Freund (2007) presented a novel approach to measuring heat transfer coefficients with infrared thermography by generating a periodic heat flux with a laser or halogen light. His method relied on measuring the phase lag between temperature and heat flux. The method was employed on a wide range of applications and had close agreement with absorption and liquid crystal based methods. The method has many advantages, but requires a great deal of post processing.

This paper describes a non-intrusive method of determining the air side heat transfer coefficient acting on a rotating body by using infrared thermography. This methodology which allows air side heat transfer to be measured without requiring heater foil or other instrumentation to be applied to the surface of interest and instead using a step change in air temperature to calculate local heat transfer. Subsequent post processing of the infrared video allows heat transfer to be relatively easily calculated. Consequently, the non-intrusive nature of this method makes it well suited for analyzing heat transfer bodies in motion, as well analyzing multiple bodies without modifications to the experimental instrumentation.

2. CONCEPT

The idea behind the proposed method comes from the conservation of energy and is most easily explained with an assumption that there is negligible temperature gradient within the solid material in the direction normal to the surface of interest. This is commonly referred to as the "lumped capacitance" approach, but as will be shown later this can be expanded on to cover many objects and their respective surfaces. The temperature assumption is an important simplification in that it assumes that the temperature below the surface is the same as the surface temperature. The rate heat is absorbed by the air and energy is released by the object are given in the left and right hand sides of Equation 2, respectively. The heat absorbed by the air by heat transfer is given by Equation 1 multiplied by the surface area of the object (A). This is equal to the energy removed from a body with volume (V) per unit time (t), which is based on the temperature of this volume as well as the density (ρ) and specific heat (c).

$$-hA_s(T - T_\infty) = \rho V c \frac{dT}{dt} \tag{2}$$

By knowing the object's initial temperature (T_i) which happens at time equals zero and by rearranging and

integrating this equation we arrive at an Equation 3.

$$\frac{T - T_\infty}{T_i - T_\infty} = e^{-\left(\frac{hA_s}{\rho V c}\right)t} \tag{3}$$

The parenthetical statement in the exponential of Equation 3 is the inverse of the thermal time constant (τ). In an experiment, if the body temperature with respect to time and the air temperature are known, then thermal time constant can be calculated by taking the natural logarithm of both sides of the equation and using least squares fitting an exponential curve between the quotient on the left hand side and time.

For a given object of known material properties and known temperature decay, it should be possible to determine the ratio of convective heat transfer coefficients directly. However, it should be noted that in a relatively limited range of temperatures, the area, density, volume, and specific heat for a solid object are nearly constant. This means that for a given object, only the convective heat transfer coefficient changes when operating conditions, such as velocity, are changed. This allows calibration when properties are unknown because the ratio of the inverse of thermal time constants as shown in Equation 4 where the naught subscript (*0*) denotes results from a calibration procedure.

$$\frac{h}{h_0} = \frac{\tau_0}{\tau} \tag{4}$$

This assumption that the temperature gradient is small is valid so long as the Biot number is small. The Biot number relates the rates of convective heat transfer on the surface of the object to conductive heat transfer within the object. In general, the Biot number (*Bi*) is given by Equation 5, where L_c is the characteristic length and *k* is the thermal conductivity of the solid object. For a thin planar-like object, the characteristic length is half the thickness of the material.

$$Bi = \frac{hL_c}{k} \tag{5}$$

Assuming Biot number must be about an order of magnitude smaller than unity, it is important to understand which geometries and conditions which would fulfill this condition. For HVAC&R heat exchangers, the air side convective heat transfer coefficient is generally on an order no greater 100 W/m^2. Polymeric materials have thermal conductivity on the order of 0.1 W/m-K with metals and ceramics generally being more conductive. Therefore, for the vast majority of combinations of engineering materials and air convective heat transfer coefficients, the preceding methodology will be applicable for geometries up to 0.1 mm thick.

While this lumped capacitance type modeling is relatively easy to demonstrate, the applicability may be a bit limited in utility. Analysis from Schneider (1955) was used in the text by Incropera and Dewitt (2002) to show that for a plane wall with Fourier numbers greater than 0.2 that "the time dependence of the temperature at any location with the wall is the same as that of the midplane temperature." This statement is generally true, however at smaller Fourier numbers, higher order eigenvalues cannot be neglected. For the sake of the method being discussed, this means that the time constant may relate back to a slightly more complex set of parameters. In this case, the time constant becomes expressed by Equation 6. In the case of a small Biot number, it can be shown that these time constants give essentially the same solution.

$$\frac{1}{\tau} = \zeta_1^2 \frac{k}{\rho c L_c^2} \tag{6}$$

Where ζ_1 is the first eigenvalue of $\zeta_n tan\zeta_n = Bi$

This equation has the unfortunate effect of making the time constant no longer linearly proportional with Biot number, and hence on the convective heat transfer coefficient. However, since ζ_1 must be positive, there is a one-to-one correspondence to Biot number. Therefore, so long as the material properties are known and the convective heat transfer coefficient can be calibrated for one condition, then convective heat transfer at another condition can be calculated with only slightly more effort. Using tabular information from Incropera and Dewitt (2002), Figure 1 was constructed to show the relationship between ζ_1 and Biot number, which is linearly proportional to convective heat

transfer coefficient. It can be seen that for the planar shape discussed, and also for an infinite cylinder, that for large values of ζ_1, that the Biot number is relatively insensitive. At such high Biot numbers, the methodology will work poorly, because the surface temperature will equal the air temperature too quickly to be able to get sufficient temporal resolution of temperature decay and due to the steep thermal gradient to the core of the surface's object. However, the approximate solution to the plane wall with convection based approach still allows for the application of a very similar method to a range of Biot numbers up to about 5, rather than just to 0.1.

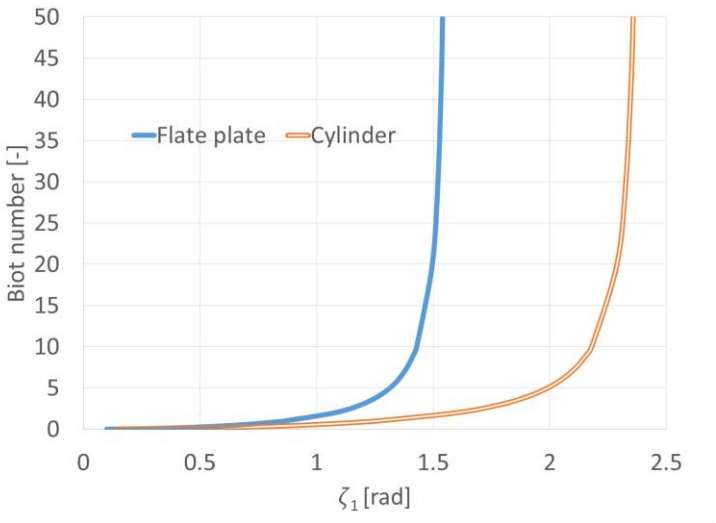

Figure 1: Relationship between eigenvalue appearing in thermal time constant to Biot number

To simplify calculations, the temperature can be non-dimmensionalized using Equation 7.

$$\theta = \frac{T - T_\infty}{T_0 - T_\infty} \tag{7}$$

Using the non-dimmensionalized temperature, and combining Equations 3 and 6, we are able to arrive at Equation 8. The thermal time constant, which is the parenthetical term, can be solved for by applying a fit to the time dependent non-dimmensionalized temperature. Once the time constant is determined, and assuming material properties are known, the value of ζ_1 can be solved for. Biot number, and subsequently heat transfer coefficient, can be found using Equations 5 and 6.

$$\theta = e^{-\left(\zeta_1^2 \frac{k}{\rho c L_c^2}\right)t} \tag{8}$$

Recall, when Biot number is less than 0.1, this solution arrived at via Equation 8 approaches the solution of the lumped capacitance approximation given by Equation 3. While very similar to Equation 3, Equation 8 is more widely applicable because it accounts for a thermal gradient existing within the object of interest, particularly in the direction normal to the surface. Equation 8 can be used to determine the convective heat transfer coefficient for Biot numbers greater than 0.1 so long as Fourier number is greater than 0.2. At smaller Fourier numbers the relationship given by Equation 9 is no longer sufficient so higher order eigenvalues would also need to be used.

$$\zeta_1 tan\zeta_1 \cong Bi \tag{9}$$

3. METHODOLOGY

Based on the concept outlined in Section 2, the basic methodology is to allow the object of interest to come to equilibrium with surrounding air, then impose a step change in air temperature, and with the use of an infrared camera, track the local decay of temperature. Using least squares curve fitting and a numerical solver, the thermal time constant can be easily calculated. The convective heat transfer coefficient is calculated from the comparison of

the measured thermal time constant to the thermal time constant at a condition with a known convective heat transfer coefficient.

3.1 Instrumentation

A few key pieces of instrumentation are needed in order to utilize the proposed methods.

Because it is necessary to measure the step change in air temperature, it is necessary to measure air temperature with fast responding instrumentation. Due to their low thermal mass, a grid of bare, welded thermocouple probes is one of the faster responding electrical temperature detectors.

Surface temperature can be precisely measured at regular time intervals with an infrared video camera. While the accuracy of many infrared cameras is often poor (2K) due to emissivity of the object of interest, flat field temperature uniformity of the bolometer, and other optical unknowns, the precision of infrared cameras is generally very good (typically 50mK). Precision is of greater importance for these experiments because the starting and ending temperatures in each thermal decay cycle is corroborated with the air thermocouple measurements.

Synchronous recording of air temperatures and surface temperatures recorded with infrared is also necessary to determine the temperature difference which is driving the heat transfer. This can be done with time stamping if machine times can be verified, but preferably the same machine is used to collect both sets of data. While ideally the air temperature undergoes a step change, some lag or transition period is experienced and must be accounted for.

3.3 Calibration procedure

If material properties and critical length, which is the volume per surface area (e.g. half the thickness of a planar object), are well characterized, then no calibration of the object of interest is necessary. This is because all values of surface temperatures are measured experimentally which allows for the calculation of the thermal time constant. As all other values (material properties and geometry) in the thermal time constant are known, no calibration is necessary.

However, this method also allows for determining the air side convective heat transfer coefficient at one condition based on knowing the convective heat transfer coefficient at another condition. Two different calibration procedures have been tried and yielded very similar results.

One option, is to use finite element modeling to simulate the effect of a step change. The output of this simulation should be the surface temperature of the object as a function of time. The numerical method requires knowing the material properties and the geometry of the object to be used in the test. Once the geometry and property information is input to the finite element software, boundary conditions must be input. Because the idea is to understand how the object responds to a step change in air temperature similar boundary conditions should be input to the finite element software. While it may be possible to directly impose an air temperature and a convective heat transfer coefficient, this requires information about the convection in the air. So instead, it is believed to be better to impose a uniform heat flux on the surface. While a uniform heat flux will almost certainly not be found in the subsequent experiments, a uniform heat flux is a very simple boundary condition to utilize for the numerical simulation and is handy for the eventual analysis of the experiments. Knowing how surface temperature responds to a given heat flux allows straightforward analysis of the experimental data because heat flux is convective heat transfer coefficient divided by the temperature difference given in Equation 1. For relatively planar shapes, the procedure can be solved numerically without going through the effort of finite element analysis as solutions for surface temperature for constant heat flux boundary conditions already exist.

The second option is to calibrate by performing the experimental operating procedure at a condition where the heat flux can be well known. One advantage of this calibration is that material properties and object geometry do not need to be known. However, the application of a known heat flux can prove challenging. Free convection or other low speed flows may be useful for calibration, but can lead to large uncertainties when used with high speed flows. Other modes of heat transfer to or from the surface, such as radiation heat transfer may prove to be more reliable for calibration.

3.3 Experimental operating procedure

The basic procedure is to apply a series of step changes in temperature and record surface and air temperatures with an infrared camera. To impose the step change in air temperature it is advantageous to have a method for drawing air from either a cold or warm air stream. This is because electric heaters, refrigerant-to-air, or coolant-to-air heat exchangers generally do not provide a sharp temperature transition. Fast moving louvers or an easily movable air heater work well to provide the step change. In short, it is necessary to have access to two air streams which are at different temperatures.

The surface of the object of interest should initially be in equilibrium with an air stream, either the warm or the cold one. Data collection of air temperature with the thermocouples, infrared video, and any other parameters (e.g. air flow rate) which are of interest in the experiment should be started. Then, the step change in temperature should be imposed by switching to the other air stream. Data collection could continue for about the time determined to be the thermal time constant in the calibration phase, assuming that a low convective heat transfer was imposed. If there is sufficient storage, data could be recorded until the surface temperature reaches the new air temperature. Once equilibrium is reached at the new temperature level, the process can be repeated by returning to the original temperature level.

3.4 Data processing and analysis

There are five major steps to data processing. All of these analysis steps have been automated by the author in a Matlab script, but these tasks can be accomplished in any number of software packages.

The first step is to relate pixel intensity values to temperature. While some infrared cameras produce an array of temperature values, many require connecting pixel values to temperature. Generally, the camera manufacturer has documentation on the specific process for connecting pixel values to temperature. It should be noted for cameras for which mapping is not available that pixel intensity may not be proportional to temperature. For any infrared camera it is good to have a known temperature somewhere in the field of view for comparison purposes.

The second step is to locate the region of interest in each frame of the video and to identify a grid of locations within the region of interest. The region of interest is the location of the heat transfer surface. The region of interest can be identified with the use of edge detection code, or could be done manually. The grid of locations could be each individual pixel within the region of interest or it could be coarser grid if there is less need for spatially precise results.

The third step is to go image-by-image and build an array of dimensionless temperature values at each grid position with respect to time. The time should be shifted so that time equals zero corresponds to the time when the step change in temperature was applied. Data from before the step change is not used in the analysis other than to serve as a check of temperature calibration. If plotted, with time on the abscissa and temperature on the ordinate, the temperature decay should be clearly visible and should be steepest near time equals zero and approach the air temperature.

The fourth step is to perform a least squares curve fit on the logarithm of the dimensionless temperature with respect to time, which is to say solving Equation 8.
While the convective heat transfer coefficient cannot be shown with a single equation, the calculations are rather straightforward computationally. An example set of results is given in Section 5 of this paper.

4. ACCURACY

Air side convective heat transfer measurements are often difficult even with dedicated heat flux sensors and more conventional techniques. The proposed methodology is on par in terms of accuracy with many other methods.

Measurement uncertainties for the instruments used in the author's experiments are given in Table 1. These numbers are relatively typical among commercially available instrumentation. It should be noted that for the infrared camera mentioned, the double the uncertainty of the infrared camera added to the accuracy of the thermocouples, which are used to check the accuracy at the steady state conditions before and after each step change.

Table 1: Instrumentation uncertainty.

Parameter	Instrumentation	Uncertainty	Units
Air temperatures	Omega T-type thermocouple	0.5	K
Surface temperature	Flir Quark infrared camera	0.6	K
Time	Raspberry Pi computer	0.440	s
Length	Tool Shop caliper	0.01	mm

From these measurement uncertainties the uncertainty of the convective heat transfer coefficient was calculated based on the method of Taylor (1994). The calculations were for a propylene fan blade having a thickness of 4mm. The uncertainty calculations assume that material properties are well known. The measured air side convective heat transfer coefficient for the condition measured was 60W/m^{2}K and a Biot number of 0.43. The method was found to be accurate to ±6.5W/m^{2}K which is ±11% of the calculated value.

5. EXPERIMENTAL UTILIZATION

Heat transfer experiments were conducted using the described methodology to understand the convective heat transfer from a rotating fan blade. The setup for the heat transfer experiments can be seen in Figure 2. The key elements of the experiment are the rotating fan blade (seen in foreground) and the rotating infrared imaging system (seen in the background), which are driven by timing belts from a single motor-driven shaft. The rotation of the fan blade and camera were synchronized to take real-time measurement during rotation while eliminating blurring caused by the relatively long exposure time of the camera. The imaging system includes the infrared camera (FLIR Quark) ,a frame grabber, microcomputer (Raspberry Pi), and battery. The fan blade as well as the entire infrared image acquisition system are mounted in a duct which allows the temperature to be changed by redirecting hot and cold air streams so as to provide an approximate step change in air temperatures.

Figure 2: Laboratory facility for measuring air side heat transfer coefficients of a rotating fan blade

An example frame from the experiments is shown in Figure 3. In this infrared image colder regions appear in blue while warm regions appear as orange. The small cyan dots on the fan blade are the grid of points used in determining local heat transfer coefficients. These points were automatically placed by the analysis software at various axial and radial positions on the fan blade after detecting the outer, inner, leading, and trailing edges of the fan blade.

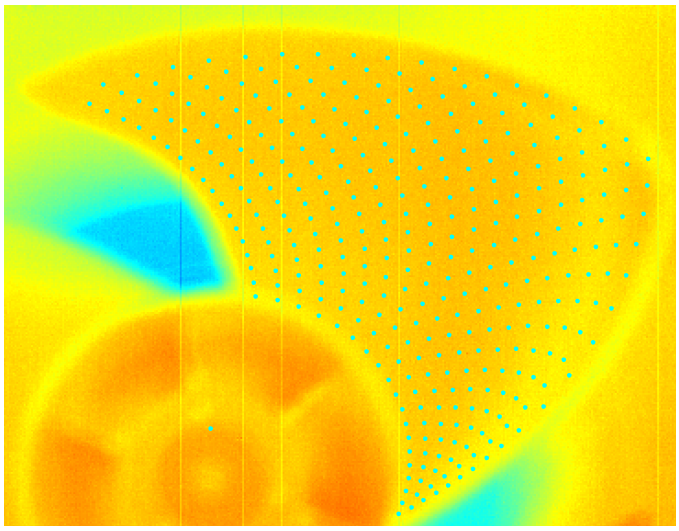

Figure 3: Example infrared image with marks denoting location of measurement grid

At each of these points, the temperature transitions from hot to cold and vice versa as the air stream temperature is changed. This allows the creation of the plot given in Figure 3. It can be seen that each temperature undergoes an approximately exponential decay in temperatures after the air temperature is changed at approximately 10 and 1100 s. The data here is calculated directly from the pixel values and what the camera manufacturer refers to as "Planck's constants". As can be seen the temperature profile at the steady state conditions is not uniform as would be expected. This scatter in temperatures is due almost exclusively calibration issues related to this particular camera, laboratory style infrared cameras should have a scatter of less than 2K. The scatter in temperatures necessitates the calibration of individual temperature measurements. Also, prior to calculation of the thermal time constant it is necessary for the data set to be split into two sections, each of which begins with the step change in air temperature and ends prior to the next transition. Scaling the temperatures and windowing the time interval were accomplished automatically by the analysis code.

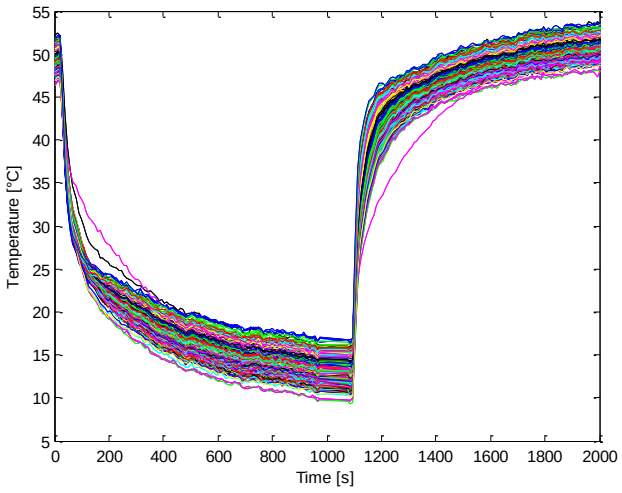

Figure 4: Temperature profiles with respect to time for each grid location

Once these temperatures at each grid location have been appropriately scaled and times have be windowed, it is possible to calculate the thermal time constant by a least squared curve fit of Equation 8. Based on material properties, or on the calibration methods described in Section 3.3, it is possible to use a numerical solver to calculate the value of ζ_1 from the thermal time constant as shown by Equation 6. In the case of this work, material properties were known, but the numerical simulation was used to calibrate the procedures since the shape of the fan blade was

relatively complex. From there, the Biot number and convective heat transfer are calculated Equations 5 and 6. An example of the convective heat transfer coefficient for the surface of the fan blade at various conditions is shown in Figure 5. The highest of the convective heat transfer coefficients shown was found when the fan blade was rotating at 860 RPM. The lowest convective heat transfer coefficient shown is for natural convection. Between these cases is with the fan blade fixed but with forced convection.

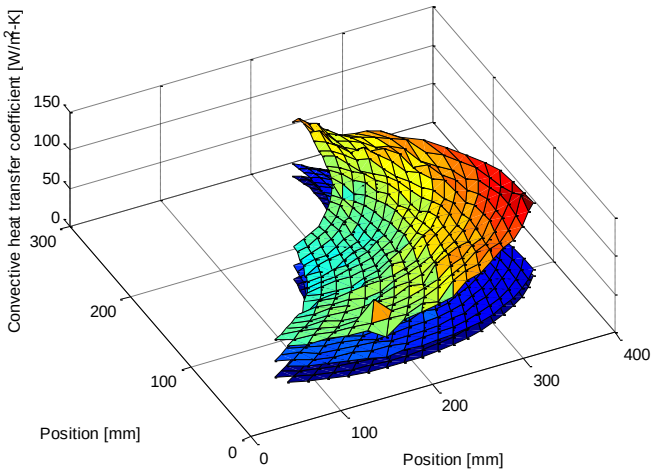

Figure 5: Calculated convective heat transfer coefficients for three operating conditions

Once convective heat transfer coefficients are known at various positions, these coefficients can be fitted to be used in analysis. This would typically be done by non-dimmensionalizing heat transfer coefficient via the Nusselt number using the Buckingham Pi theorem to arrive at an equation which incorporates Reynolds, Prandtl, or other terms. Ongoing research will hope to validate the method by comparing experimental results for some archetypal geometry and flow conditions.

6. CONCLUSIONS

A new method for measuring heat transfer has been presented, where the temperature decay of a heat transfer body heated or cooled by airflow is measured with infrared thermography to determine the local heat transfer coefficients. The method differs from previous measurement techniques in that it eliminates the need to adhere heated foils, thermocouples, liquid crystals, or heat flux sensors to the surface of interest. Consequently, it allows for a faster screening of different heat transfer surface geometries. This method was used in this study to determine the heat transfer coefficients of a rotating fan blade; this method has an advantage for rotating and other moving heat transfer surfaces in that it eliminates the need for expensive slip rings or wireless high precision data loggers. The downside of this method is lower accuracy (about 11% for the case demonstrated), requires either calibration or known material properties, and more complex mathematical analysis.

The experimental method was described in theory, errors were calculated when utilizing relatively typical laboratory instrumentation, and an example experimental method was shown.

NOMENCLATURE

A	area	(m^2)
Bi	Biot number	(-)
c	specific heat	(J/kgK)
h	convective heat transfer coefficient	(W/m^2K)
k	thermal conductivity	(W/mK)
L	length	(m)
q"	heat flux	(W/m^2)
T	temperature	(K)

t	time	(s)
V	volume	(m^3)
ζ	eigenvalue solution	(radians)
θ	dimensionless temperature	(-)
ρ	density	(kg/ m^3)
τ	thermal time constant	(s)

Subscript

c	characteristic
i	initial
s	surface
∞	fluid, bulk
0	known, calibrated
1	first

REFERENCES

Blair, M. F. & Anderson, O. L. (1989), *The effects of Reynolds number, rotor incidence angle and surface roughness on the heat transfer distribution in a large-scale turbine rotor passage.* NASA Marshall Space Flight Center: National Aeronautics and Space Administration.

Freund, S., (2007) *Local heat transfer coefficients measured with temperature oscillation IR thermography*. Hamburg: University of the Federal Armed Forces Hamburg.

Incropera, F. P. & DeWitt, D. P. (2001), *Fundamentals of Heat and Mass Transfer, 5th Edition*. New York, NY: John Wiley and Sons.

Schneider, P. J. (1955), *Conduction heat transfer*. Reading, MA: Addison-Wesley.

Taylor B.N. & Kuyatt, C.E. (1994), *Guidelines for Evaluating and Expressing the Uncertainty of NIST Measurement Results*, Gaithersburg, MD: National Institute of Standards and Technology.

ACKNOWLEDGEMENT

Funding for this work was provided by the Building Energy Efficiency Frontiers and Incubator Technologies funding opportunity from the Department of Energy's Building Technologies Office (DE-FOA-0001027).